


ORIGINAL ARTICLE

MicroRNA-324-3p inhibits osteosarcoma progression by suppressing PGAM1-mediated aerobic glycolysis

Yiping Weng^{1,2} | Weihao Duan² | Xuecheng Yu² | Furen Wu^{2,3} | Daibin Yang^{2,3} |
 Yuqing Jiang² | Jingbin Wu² | Muyi Wang² | Xin Wang² | Yifei Shen²  |
 Yunkun Zhang² | Hua Xu¹

¹State Key Laboratory of Bioelectronics, School of Biological Science and Medical Engineering, Southeast University, Nanjing, China

²Department of Orthopedics, The Affiliated Changzhou Second People's Hospital of Nanjing Medical University, Changzhou Medical Center, Nanjing Medical University, Changzhou, China

³Graduate School, Dalian Medical University, Dalian, China

Correspondence

Yifei Shen and Yunkun Zhang, Department of Orthopedics, The Affiliated Changzhou Second People's Hospital of Nanjing Medical University, Changzhou Medical Center, Nanjing Medical University, 68 Gehu Middle Road, Changzhou, 213003, Jiangsu province, China.

Email: nydshenyifei@163.com and njmyunkunzhang@163.com

Hua Xu, State Key Laboratory of Bioelectronics, School of Biological Science and Medical Engineering, Southeast University, 2 Si Pai Lou, Nanjing, 210096, Jiangsu Province, China. Email: huaxu@seu.edu.cn

Funding information

Changzhou Medical Center of Nanjing Medical University, Grant/Award Number: CMCB202208 and CMCC202217; Changzhou Science and Technology Bureau, Grant/Award Number: CE20215020; the Natural Science Foundation of Xinjiang Uygur Autonomous Region, Grant/Award Number: No. 2022D01F95

Abstract

Osteosarcoma (OS) is the most common primary malignant neoplasm of the bone. Recent studies have indicated that the inhibitory effects of microRNA (miR)-324-3p could affect the development of numerous cancers. However, its biological roles and underlying mechanisms in OS progression remain unexplored. In this study, miR-324-3p expression was markedly reduced in OS cell lines and tissues. Functionally, miR-324-3p overexpression suppressed OS progression and was involved in the Warburg effect. Mechanistically, miR-324-3p negatively regulated phosphoglycerate mutase 1 (PGAM1) expression by targeting its 3'-UTR. Moreover, high expression of PGAM1 promoted OS progression and aerobic glycolysis, which were associated with inferior overall survival in patients with OS. Notably, the tumor suppressor functions of miR-324-3p were partially recovered by PGAM1 overexpression. In summary, the miR-324-3p/PGAM1 axis plays an important role in regulating OS progression by controlling the Warburg effect. Our results provide mechanistic insights into the function of miR-324-3p in glucose metabolism and subsequently on the progression of OS. Targeting the miR-324-3p/PGAM1 axis could be a promising molecular strategy for the treatment of OS.

KEYWORDS

miR-324-3p, osteosarcoma, PGAM1, therapeutic target, Warburg effect

ABBREVIATIONS: IACUC, Institutional Animal Care and Use Committee; IF, immunofluorescence; IHC, immunohistochemistry; miR, microRNA; miRNA, microRNA; OS, osteosarcoma; PG, phosphoglycerate; PGAM1, phosphoglycerate mutase 1; qRT-PCR, quantitative real-time PCR; SLC25A10, solute carrier family 25 member 10.

Yiping Weng, Weihao Duan, and Xuecheng Yu contributed equally to this work and share first authorship.

This is an open access article under the terms of the [Creative Commons Attribution-NonCommercial-NoDerivs](https://creativecommons.org/licenses/by-nc-nd/4.0/) License, which permits use and distribution in any medium, provided the original work is properly cited, the use is non-commercial and no modifications or adaptations are made.

© 2023 The Authors. *Cancer Science* published by John Wiley & Sons Australia, Ltd on behalf of Japanese Cancer Association.

1 | INTRODUCTION

Osteosarcoma is recognized as the most common form of bone cancer and has a great propensity for pulmonary metastasis.¹ Osteosarcoma presents most frequently in children and adolescents.² Notably, in patients with localized OS, long-term survival rates have reached 60% due to the application of neoadjuvant chemotherapy and surgical resection.^{3,4} However, there has been no major improvement in the overall survival rates of such patients in the past three decades.⁵ Therefore, a better understanding of the potential molecular mechanisms of OS is essential to identify therapeutic targets for targeted therapy.

MicroRNAs are evolutionarily conserved noncoding RNAs that promote mRNA degradation or translational inhibition at the post-transcriptional level.^{6,7} There is considerable evidence that miRNAs and their biogenesis machinery are involved in tumor growth, metastasis, angiogenesis, and immune evasion.⁸⁻¹⁰ Furthermore, accumulating evidence has established that deregulated miRNAs act as tumor suppressors or oncogenic factors, and some of them have the potential to become novel diagnostic and prognostic biomarkers.^{11,12} In particular, miR-324-3p, a 23-nt-long miRNA, is located on chromosome 17p13.1. Recent studies have reported that miR-324-3p acts as a tumor suppressor and affects the progression of numerous tumors. For example, upregulation of miR-324-3p enhanced ferroptosis of non-small-cell lung cancer cells by inhibiting GPX4 directly.¹³ Another study reported that miR-324-3p has the potential to become a novel therapeutic target by targeting WNT2B in nasopharyngeal carcinomas.¹⁴ However, whether miR-324-3p regulates OS progression and its regulatory mechanisms remains largely unknown.

The Warburg effect – considered as a key metabolic hallmark of cancer – is a metabolic alteration stimulated by aerobic glycolysis that suppresses oxidative phosphorylation.¹⁵ This metabolic reprogramming phenomenon is present in multiple cancers, and it markedly facilitates cancer proliferation, aggressiveness, and therapeutic resistance.¹⁶⁻¹⁸ According to a previous study, this effect is also a characteristic of OS that could be targeted therapeutically.¹⁹ Additionally, miRNAs have been suggested to be the important regulators of aerobic glycolysis and tumorigenesis in various cancers. Moreover, Fong et al. reported that miR-122 overexpression suppresses breast cancer progression by regulating glucose utilization.²⁰ Guo et al. reported that miR-199a-5p regulates cancer proliferation and glucose metabolism by targeting HK2 in liver cancer.²¹ However, whether miR-324-3p participates in glycolysis and energy metabolism in OS remains unclear.

In the present study, we found that miR-324-3p was expressed at low levels in OS and that its overexpression hindered OS progression by inhibiting aerobic glycolysis. Mechanistically, we discovered that *PGAM1*, a critical glycolytic coding gene, was suppressed by miR-324-3p, which inhibited aerobic glycolysis. Briefly, these findings indicate that targeting the miR-324-3p/*PGAM1* axis could provide a promising molecular strategy for the treatment of OS.

2 | MATERIALS AND METHODS

2.1 | Cell culture

The human OS cell lines U-2OS, 143B, MG63, and MNNG-HOS and the human osteoblast cell line hFOB1.19 were obtained from the Cell Bank of the Chinese Academy of Sciences. Osteosarcoma cells were incubated at 37°C in humidified air containing 5% CO₂, whereas hFOB1.19 cells were maintained at 34.5°C with 5% CO₂ in a humidified atmosphere. All cells were cultured in a medium containing 10% FBS and 1% penicillin–streptomycin.

2.2 | Quantitative real-time PCR analysis

Total RNA was isolated from different cell lines and reversed transcribed to cDNA according to the manufacturer's instructions (Vazyme). The qRT-PCR analysis was carried out as previously described.²² 18S and U48 small nuclear RNAs were used as internal controls for mRNA normalization. Their relative expressions were calculated using the $2^{-\Delta\Delta Ct}$ method.

2.3 | Transfection assay

For siRNA transfection, *PGAM1* siRNA and negative control siRNA were synthesized by GenePharma. Furthermore, the cells were transiently transfected using jetPRIME (Polyplus Transfection) according to the manufacturer's instructions. The target sequences for *PGAM1* siRNAs are as follows: si-*PGAM1*-1, 5'-GUCCUGUCCAA GUGUAUCUTT-3' (sense), 5'-AGAUACACUUGGACAGGACTT-3' (antisense); and si-*PGAM1*-2, 5'-CCACAUCUGUAGACAUCUUTT-3' (sense), 5'-AAGAUGUCUACAGAUGUGGTT-3' (antisense).

Plasmids containing miR-324-3p or *PGAM1* and the negative control plasmids were purchased from OBio Technology. Furthermore, the constructed plasmids were packaged with the lentivirus expression system using HEK 293T cells, and viral titers were determined. To obtain stable miR-324-3p-overexpressing or *PGAM1*-overexpressing cells, target cells were seeded on 6-well plates and coinfecting with 1×10^8 lentivirus-transducing and polybrene (Sigma). After 72h, the infected cells were screened using 2.5 µg/mL puromycin. Furthermore, western blotting and qRT-PCR were undertaken to evaluate the transfection efficiency.

2.4 | Western blot assay

Western blotting was carried out as previously described.²² Briefly, the supernatant was collected after centrifugation at 12,000g. Subsequently, the protein samples were mixed with protein loading buffer, separated using gel electrophoresis, and then transferred to the membrane. The membranes were incubated at 4°C overnight with primary Abs; subsequently, they were incubated with secondary Abs

at room temperature for 1 h. The bands were visualized by enhanced chemiluminescence. Antibodies against β -actin (1:10000, ab8226; Abcam), PGAM1 (1:2000, ab129191; Abcam), Bcl-2 (1:1000, #4223; CST), Bax (1:1000, #5023; CST), caspase-3 (1:1000, 19,677-1-AP; Proteintech), and cleaved caspase-3 (1:1000, A11021; Abclonal) were used.

2.5 | Cell counting and colony formation assays

Cell viability was measured using a CCK-8 assay kit (Share-bio) according to the vendor's instructions. Subsequently, the transfected cells were seeded into 96-well plates (3×10^3 cells/well). Finally, the absorbance was measured at 450 nm using a microplate reader (Bio-Rad Laboratories) at 0, 24, 48, 72, 96, and 120 h.

For colony formation assays, the cells subjected to various treatments were seeded into a 6-well plate at a concentration of 1000 cells/well and incubated for 2 weeks. After washing with ice-cold PBS, these cells were fixed with 4% paraformaldehyde. Finally, cell colonies were imaged and counted after staining with crystal violet.

2.6 | Migration and invasion assays

Cell migration and invasion ability were assessed using Transwell assays. For the migration assay, 3×10^4 cells treated with U-2OS and 143B were added to the upper chamber with serum-free medium. The medium supplemented with 10% FBS was then added to the lower chamber as a chemoattractant. For the invasion assay, Transwell inserts (24-well inserts, 8- μ m pore size; Corning) were coated with diluted Matrigel (BD Biosciences). After incubating for 48 h, the cells were fixed with 4% formaldehyde. Finally, cells that had migrated or invaded across the membrane were counted and imaged using an inverted microscope (Olympus) after staining with 0.1% crystal violet.

2.7 | Mouse xenograft model

All animal experiments were approved by the IACUC of Jiangsu Science Standard Medical Testing Co., Ltd (IACUC22-0098). Female BALB/C nude mice were subcutaneously injected with 1.5×10^6 transfected cells at the age of 5 weeks ($n = 5$ mice in each group). Tumor sizes were estimated every 5 days with caliper measurements and calculated using the following formula: $\text{width}^2 \times \text{length} \times 0.5$. After 20 days of OS cell injections, all mice were killed, and tumors were isolated and weighed.

2.8 | Immunohistochemistry staining

The IHC assay was carried out as previously described.¹⁹ To detect cell proliferation of xenograft tumor tissues, IHC staining was undertaken with Abs of Ki-67 (GB13030; Servicebio), at 1:200 dilutions.

Furthermore, cell apoptosis of xenograft tumor was evaluated using a TUNEL kit (Roche). All images were visualized using a fluorescence microscope (Carl Zeiss).

2.9 | Fluorescence in situ hybridization

A microarray of tissues from 40 patients with OS was obtained from Alena Biotechnology Co., Ltd. The OS tissue sections were hybridized with the miR-324-3p and PGAM1 probes (Servicebio) and FISH was carried out as previously described.¹⁹

2.10 | Metabolic assays

The extracellular acidification rate and oxygen consumption rate were measured using an XF96 metabolic flux analyzer (Seahorse Biosciences) as previously described.²² Cellular ATP levels were quantified using an ATP assay kit (Promega), and extracellular lactate levels were determined using a lactate assay kit (BioVision) according to the vendor's instructions.

2.11 | Flow cytometry

Apoptosis was evaluated using the annexin V-FITC/propidium iodide apoptosis assay kit (Share-bio). Cells were harvested after 72 h of transfection and were processed according to the manufacturer's instructions. Apoptosis was determined by flow cytometry using a BD Biosciences flow cytometer.

2.12 | Luciferase activity assays

Wild-type and mutant PGAM1 were created and cloned into the pmir vector and cotransfected into OS cells using Lipofectamine 2000 (Invitrogen). Cells were collected after 48 h of transfection, and luciferase activities were measured using the Dual-Glo Luciferase Assay System (Promega).

2.13 | Database analysis

Data regarding potential miR-324-3p-target genes were obtained from the online software StarBase (<http://starbase.sysu.edu.cn>) and miRDB (<http://www.mirdb.org>).

2.14 | Bioinformatic analysis and survival analysis

The gene expression microarray data from the GSE65071 dataset were directly obtained from GEO (<http://www.ncbi.nlm.nih.gov/geo/>), comprising 20 OS samples (10 localized and 10 metastatic)

and 15 normal samples. Gene expressions were normalized by the quantile normalization method using the `normalizeBetweenArrays` function in the `limma` package from BioConductor in R software version 4.2.1 (R Development Core Team, Vienna, Austria). Differential expression was determined in R using the `limma` and `DESeq2` packages from BioConductor (<https://www.bioconductor.org/>).

The gene expression data and survival information of 85 patients with OS in the TARGET-OS database (<https://portal.gdc.cancer.gov/projects/TARGET-OS>) were generated using the UCSC Xena platform (<https://xena.ucsc.edu/>). Patients were classified into two groups according to the median gene expression: high and low expression groups. Kaplan–Meier survival curves were generated using the `survfit` and `survdiff` functions of the R survival package and visualized using the `ggsurvplot` function in the R package `survminer`. Statistical significance was calculated using the log-rank test.

2.15 | Statistical analyses

All statistical results are presented as means \pm SD. Statistical analyses were undertaken using two-tailed Student's *t*-test for comparison of different groups (GraphPad Prism, version 9.3.1 for Windows). A *p* value of less than 0.05 was considered to indicate statistically significant difference.

3 | RESULTS

3.1 | MicroRNA-324-3p is significantly downregulated in OS

To identify differentially expressed miRNA in OS, the miRNA expression profiles of GSE65071 from the GEO database were analyzed using the R package. As shown in a heatmap and volcano plot (Figure 1A,B), differentially expressed miRNAs between the OS and normal tissues were identified using R package `limma` ($\log_{2}FC > 1$ and adjusted *p* value < 0.05). Among these miRNAs, miR-324-3p was significantly downregulated in OS samples compared with normal samples (Figure 1C). To further validate these results, we evaluated the expression level of miR-324-3p in tissue samples using FISH with a specific miR-324-3p probe on the microarray of OS tissues (*n* = 40). The results indicated that the miR-324-3p expression was negatively correlated with advanced pathological staging in OS (Figure 1D,E). Furthermore, the expression of miR-324-3p in hFOB1.19 cells and OS cell lines (143B, U-2OS, MG63, and MNNG-HOS) was determined using qRT-PCR. As shown in Figure 1F, the expression of miR-324-3p was markedly lower in OS cell lines than in hFOB1.19 cells, especially in U-2OS and 143B cells. Briefly, these results confirmed that miR-324-3p expression was low in OS tissues and cells, and this might be related to the progression of OS.

3.2 | MicroRNA-324-3p significantly inhibited progression of OS in vitro

To further explore the roles of miR-324-3p in OS, stable cell lines overexpressing miR-324-3p were established, and the efficiency of overexpression was determined using qRT-PCR (Figure S1A). As shown in Figure 2A–D, miR-324-3p overexpression remarkably attenuated OS cell viability and colony formation. In addition, the results of Transwell assays revealed that miR-324-3p overexpression remarkably decreased cell migration (Figures 2E and S1B) and invasion (Figures 2F and S1C) in OS cells. Moreover, miR-324-3p overexpression significantly augmented apoptosis of OS cells (Figure 2G,H). To explore the potential mechanisms underlying apoptosis due to miR-324-3p overexpression, western blotting was used to determine the protein levels of several apoptosis-related molecules. The results indicated that the expression of proapoptotic proteins Bax and cleaved caspase-3 was upregulated, whereas that of an antiapoptotic protein, Bcl-2, was downregulated (Figure S1D). Briefly, these data highlight the crucial role of miR-324-3p in promoting apoptosis and inhibiting the proliferation, migration, and invasion of OS cells.

3.3 | MicroRNA-324-3p is related to regulation of the Warburg effect in OS cells

The Warburg effect is a well-known tumor-related phenomenon that regulates tumor promotion and progression.²³ In particular, we aimed to determine whether miR-324-3p was related to this in OS. Thus, XF96 metabolic flux analyzer was used to explore its role in reprogramming glucose metabolism in OS. As shown in Figure 3A,B, miR-324-3p overexpression clearly suppressed the glycolytic capacity of OS cells, but it simultaneously enhanced their oxidative phosphorylation capacity (Figure 3C,D). Moreover, miR-324-3p overexpression inhibited the production of lactic acid, the end product of glycolysis (Figure 3E). Furthermore, miR-324-3p overexpression increased the amount of ATP produced by oxidative phosphorylation (Figure 3F). Thus, these findings indicated that miR-324-3p is an essential regulator of the Warburg effect in OS cells.

3.4 | Phosphoglycerate mutase 1 is a direct target of miR-324-3p

To explore the potential mechanism by which miR-324-3p regulated aerobic glycolysis in OS, we used two target gene prediction algorithms, StarBase and miRDB, to identify miR-324-3p target mRNA candidates. It was found that only PGAM1 and SLC25A10 were related to aerobic glycolysis (Figure 4A). We also found that miR-324-3p overexpression remarkably suppressed PGAM1 expression in OS cells, but the expression of SLC25A10 was not altered significantly (Figures 4B,C). Furthermore, we examined the

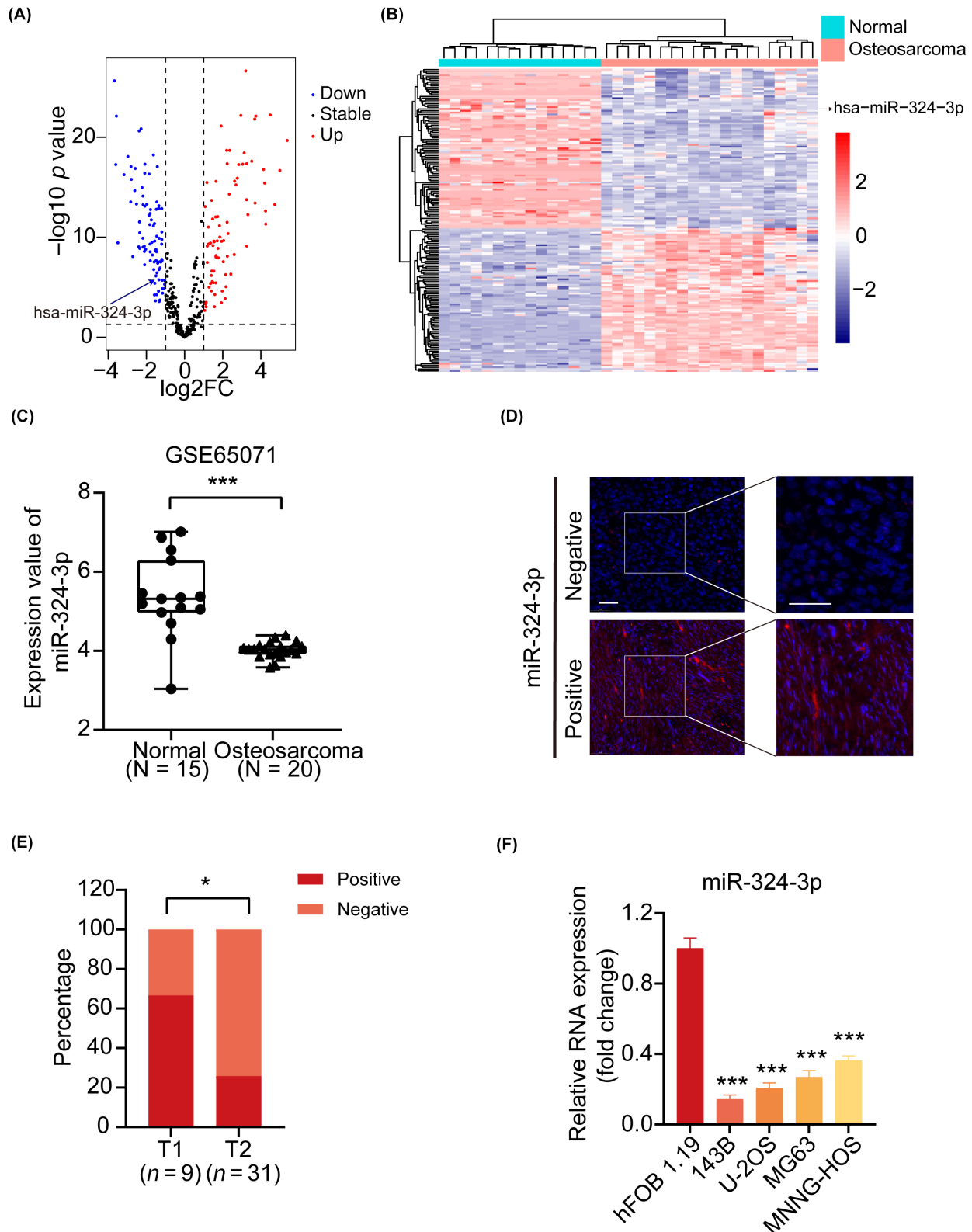


FIGURE 1 Expression of microRNA (miR)-324-3p is decreased in osteosarcoma (OS). (A) Volcano plot illustrating the differentially expressed miRNA in GEO datasets (GSE65071). (B) Heatmap showing the differentially expressed miRNA in GSE65071 obtained from the GEO database. (C) Expression of miR-324-3p in normal and OS samples of GSE65071 dataset. (D) Representative FISH images of the expression patterns of miR-324-3p in human OS tissues. Scale bar, 50 μ m. (E) Statistical analysis of FISH results based on the expression level of miR-324-3p in T1 (n = 9) and T2 (n = 31) stages in OS tissues. (F) miR-324-3p mRNA levels of U-2OS, 143B, MG63, and MNNG-HOS relative to hFOB.1.19 cells were determined using quantitative real-time PCR. Results are presented as mean \pm SD. * p < 0.05, *** p < 0.001.

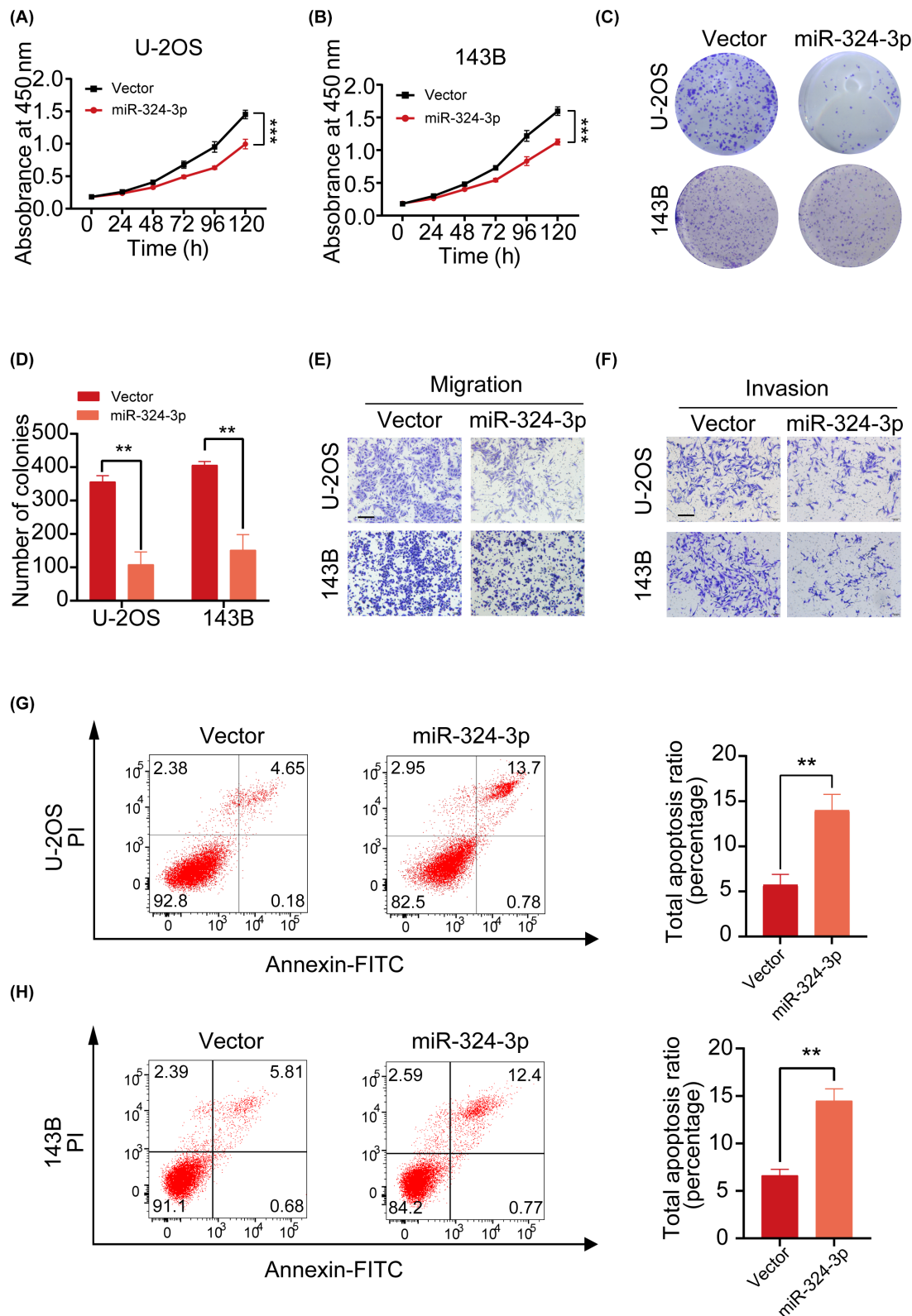


FIGURE 2 MicroRNA (miR)-324-3p suppresses osteosarcoma (OS) progression in vitro. (A, B) CCK-8 assay was used to assess the cell proliferation rate of OS cells after miR-324-3p overexpression. (C, D) Colony formation assays were used to evaluate the colony formation capacity of miR-324-3p overexpression. (E, F) Cell migration and invasion ability was detected in OS cells based on the presence or absence of miR-324-3p overexpression. Scale bar, 100 μ m. (G, H) Effects of miR-324-3p overexpression on apoptosis of OS cells were detected by flow cytometry. Results are presented as mean \pm SD. ** p < 0.01, *** p < 0.001. PI, propidium iodide.

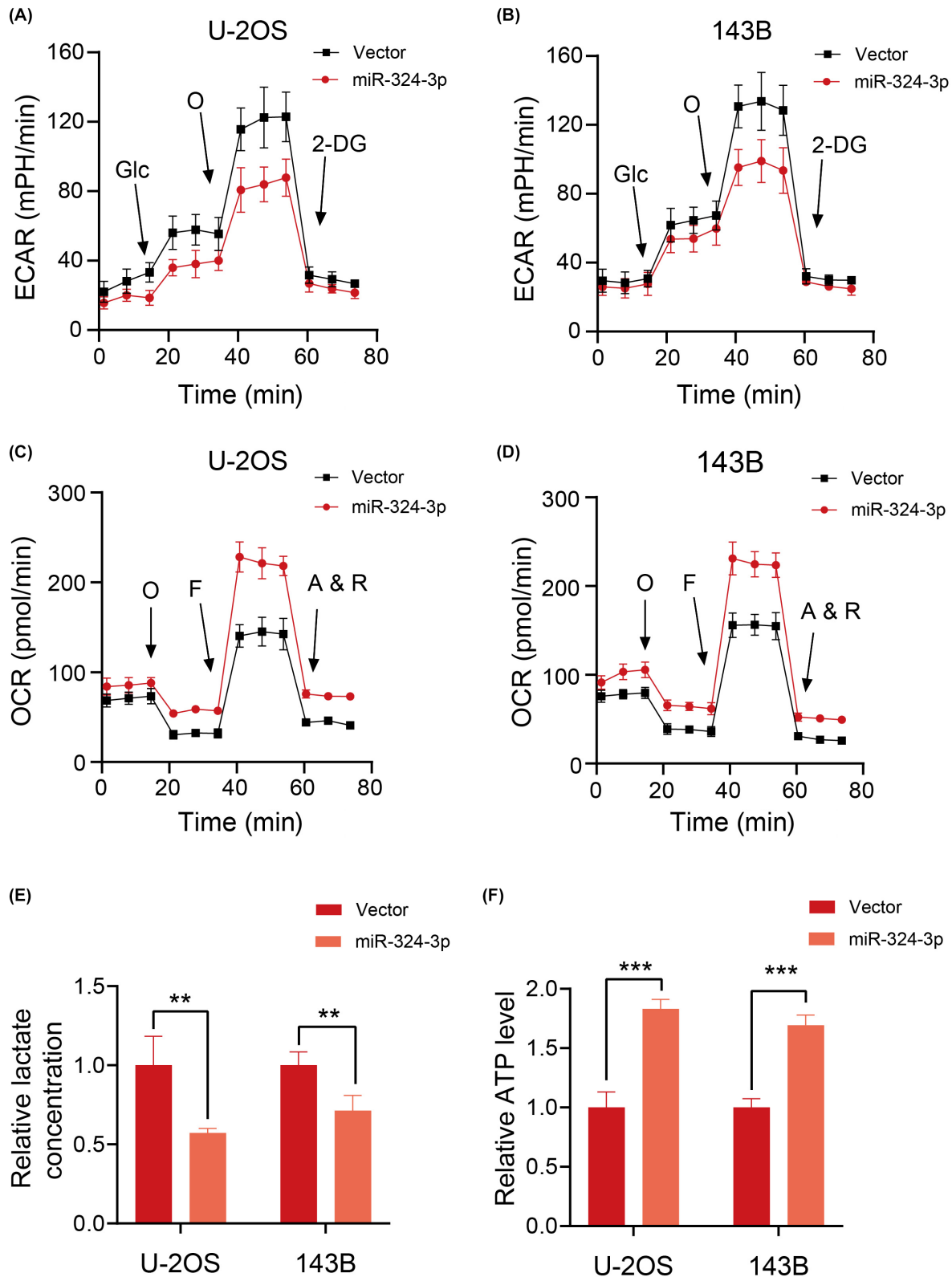


FIGURE 3 MicroRNA (miR)-324-3p inhibits aerobic glycolysis in osteosarcoma (OS) cells in vitro. (A, B) Extracellular acidification rates (ECAR) and (C, D) O_2 consumption rates (OCR) of OS cells transfected with a negative control and miR-324-3p plasmid. (E) Lactate production and (F) ATP levels validated that miR-324-3p overexpression suppressed aerobic glycolysis in OS cells. Results are presented as mean \pm SD. ** $p < 0.01$, *** $p < 0.001$. 2-DG, 2-deoxy-d-glucose; A&R, antimycin A/rotenone; FCCP, Carbonyl cyanide-p-trifluoromethoxyphenylhydrazine; Glc, glucose; O, oligomycin.

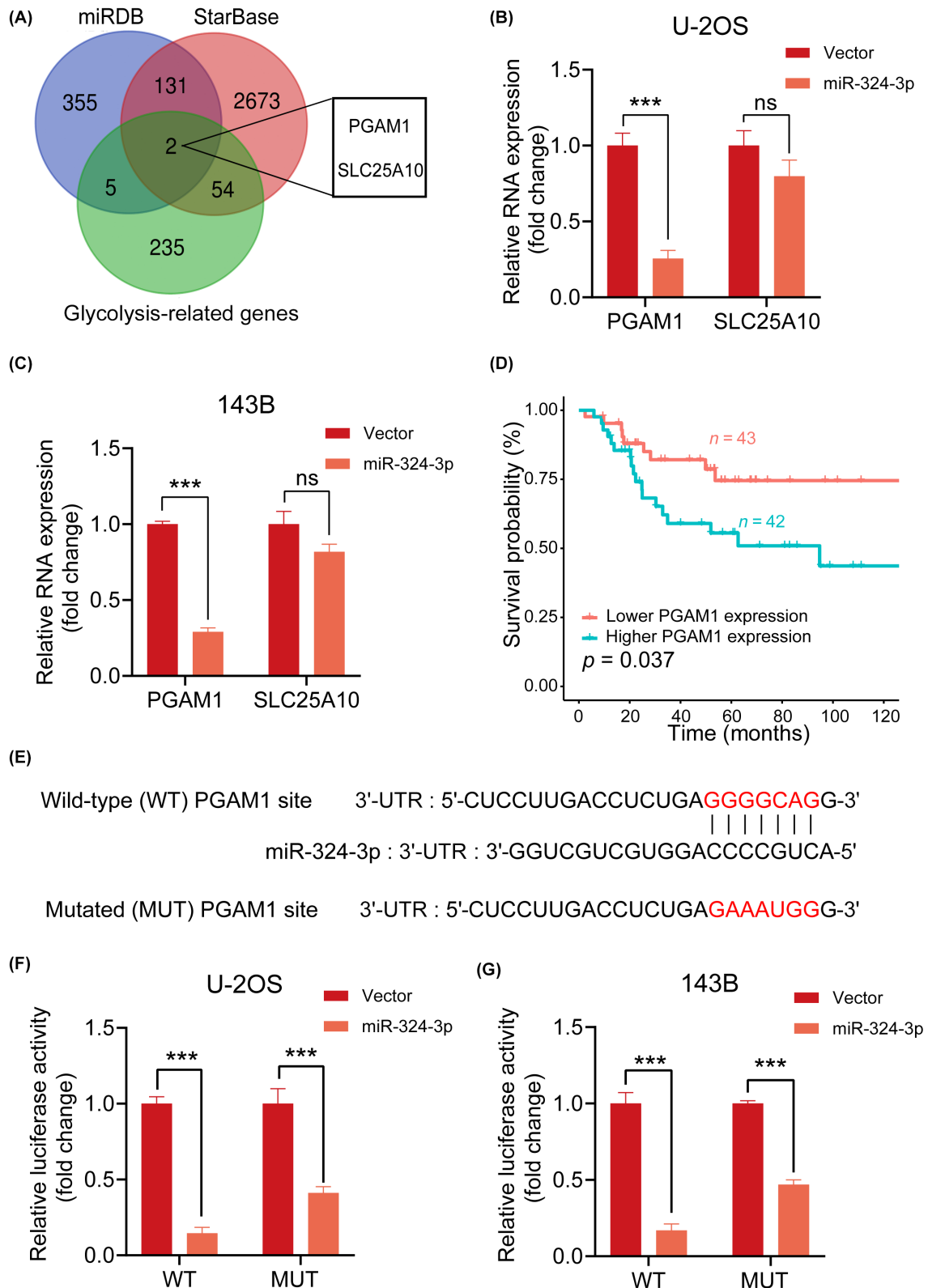


FIGURE 4 Phosphoglycerate mutase 1 (PGAM1) is an authentic target of microRNA (miR)-324-3p. (A) Venn diagram showing the predicted glycolysis-related target genes of miR-324-3p obtained from StarBase and miRDB databases. (B, C) PGAM1 and solute carrier family 25 member 10 (SLC25A10) mRNA expression in osteosarcoma (OS) cells transfected with a negative control or miR-324-3p plasmid. (D) Kaplan-Meier curves showing the association between PGAM1 expression and overall survival. (E) PGAM1 3'-UTR contains one predicted miR-324-3p binding site. (F, G) Dual-luciferase reporter assays in OS cells transfected with PGAM1 UTR WT or mutant (MUT) in combination with miR-324-3p plasmid or a negative control plasmid. Results are presented as mean \pm SD. *** p < 0.001, ** p < 0.01, ns, p > 0.05.

prognostic significance of PGAM1 expression in overall survival using the TARGET-OS dataset. As shown in Figure 4D, higher levels of PGAM1 expression were positively correlated with an adverse prognosis ($p = 0.037$), whereas SLC25A10 expression had no significant correlation with survival ($p = 0.678$) in patients with OS (Figure S2). The potential target site on PGAM1 3'-UTR for miR-324-3p is shown in Figure 4E. To demonstrate the relationship between miR-324-3p and PGAM1, luciferase reporter assays were used. As shown in Figure 4F,G, miR-324-3p markedly reduced the luciferase activity of the PGAM1-3'-UTR WT reporter but not of the PGAM1-3'-UTR mutation reporter. Overall, these findings indicated that miR-324-3p directly targets PGAM1 expression in OS.

3.5 | Phosphoglycerate mutase 1 accelerates OS cell progression by regulating the Warburg effect

As a key metabolic enzyme in glycolysis, PGAM1 has been widely known to be involved in various aspects of tumor progression. However, further studies are required to clarify whether and how PGAM1 contributes to OS progression. We initially knocked down PGAM1 by siRNA-mediated gene silencing, and the efficiency of knockdown was evaluated using western blotting (Figure 5A). Based on CCK-8 assays, PGAM1 silencing significantly attenuated OS cell proliferation (Figure 5B,C). Consistently, PGAM1 silencing substantially reduced the colony formation ability of OS cells (Figures 5D and S3A). Transwell assays revealed that PGAM1 silencing suppressed migration and invasion in OS cells (Figures 5E,F and S3B,C). In addition, as shown in Figures 5G,H and S3D, knockdown of PGAM1 specifically promoted cell apoptosis and effectively modulated the expression of the apoptosis-related markers in OS cells. Moreover, downregulated expression of PGAM1 led to decreased glycolytic capacity and increased oxidative phosphorylation capacity compared with control cells (Figure 5I,J). These findings further suggested that PGAM1 inhibited apoptosis and accelerated progression in OS cells, at least in part, by regulating the Warburg effect.

3.6 | MicroRNA-324-3p suppresses OS progression through PGAM1-mediated glycolysis

Figure 2 shows that miR-324-3p overexpression inhibits OS cell progression. To investigate whether it exerts these effects by targeting PGAM1, we cotransfected OS cells with PGAM1 overexpression lentivirus. We then verified the overexpression efficiency by western blotting (Figure 6A). The CCK-8 assays indicated that PGAM1 overexpression can partially reverse this inhibited effect on OS cell proliferation mediated by increased miR-324-3p expression levels in vitro (Figure 6B,C). Moreover, similar results were observed in the colony formation assays (Figures 6D and S4A). In addition, PGAM1 overexpression

dramatically attenuated the stimulatory effect of miR-324-3p on OS cell apoptosis, and inhibitory effect on cell migration and invasion (Figures 6E-G and S4B-E). Moreover, upregulation of PGAM1 expression in OS cells can partially recover the inhibition of the Warburg effect after enforced expression of miR-324-3p (Figure 6H-K). These results further indicate that miR-324-3p attenuated OS cell proliferation, migration, and invasion by regulating PGAM1-mediated glycolysis.

3.7 | MicroRNA-324-3p attenuates OS growth through targeting PGAM1 in vivo

To confirm whether miR-324-3p stimulates OS cell proliferation in vivo, xenograft models of OS were established in nude mice by subcutaneously injecting OS in established stable cell lines. As shown in Figures 7A,B and S5A,B, the miR-324-3p-overexpressing group showed markedly reduced tumor burden and inhibited growth of xenograft tumors compared with the control group. Nevertheless, antitumorigenic effects of miR-324-3p could be partially recovered by reintroduction of PGAM1. Subsequently, apoptosis and proliferation of cells in xenograft tumor was analyzed by Ki-67 staining and TUNEL assay, respectively. As shown in Figures 7C and S5C,D, miR-324-3p overexpression led to a significant reduction in cell proliferation and induced apoptosis in vivo, whereas PGAM1 overexpression restored this tumor-suppressor effect. Furthermore, the expression patterns of miR-324-3p and PGAM1 were established using FISH and IF staining in xenograft tumors (Figure 7D). In addition, a negative correlation between the expression pattern of miR-324-3p and PGAM1 was validated by FISH and IF analysis in OS samples of tissue microarrays (Figure 7E,F). These results further validated that miR-324-3p suppressed OS cell growth by targeting PGAM1 in vivo.

4 | DISCUSSION

In relevant published works, many studies have reported that miR-324-3p is involved in cell proliferation, apoptosis, migration, and invasion in several cancers.²⁴⁻²⁹ For example, upregulation of miR-324-3p inhibits ovarian cancer proliferation and metastasis by negatively regulating LY6K.³⁰ Moreover, previous reports have determined that the upregulation of miR-324-3p can inhibit pancreatic cancer cell growth and invasion.³¹ In the present study, bioinformatics analysis revealed that miR-324-3p expression was reduced in the OS group compared with the normal group from the GEO dataset. Consistently, in vitro and in vivo experiments confirmed that miR-324-3p was downregulated in OS cells and tissues. Moreover, miR-324-3p suppressed cell proliferation, migration, and invasion in vitro. The findings of the present study indicated that miR-324-3p acts as a tumor suppressor and plays a crucial role in the progression of OS. Furthermore, we elucidated the role of miR-324-3p in metabolic alterations in OS cells. We

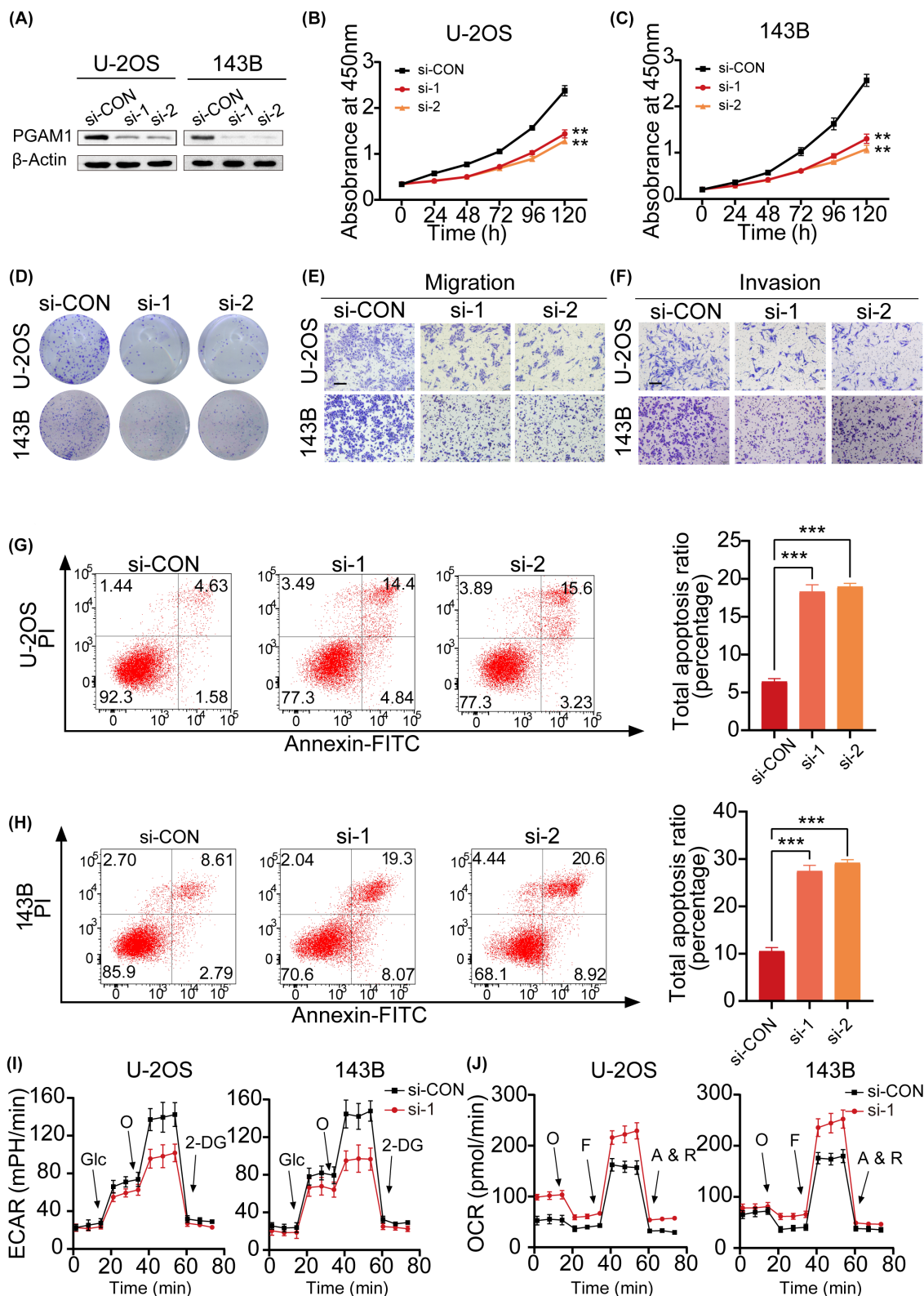


FIGURE 5 Phosphoglycerate mutase 1 (PGAM1) facilitates osteosarcoma (OS) progression and the Warburg effect in OS cells. (A) Silencing efficacy of PGAM1 siRNA in OS cells determined by western blotting. (B, C) CCK-8 and (D) colony formation assays show that silencing of PGAM1 significantly suppressed OS cell proliferation. (E, F) Transwell assay results revealed that PGAM1 knockdown inhibited cell migration and invasion ability of OS cells. Scale bar, 100 μ m. (G, H) PGAM1 silencing increased the apoptosis of OS cells. (I, J) Extracellular acidification rates (ECAR) and O_2 consumption rates (OCR) of OS cells in the si-Control (si-CON) and si-PGAM1 (si-1 and si-2) groups were detected. Results are presented as mean \pm SD. ** p < 0.01, *** p < 0.001. PI, propidium iodide.

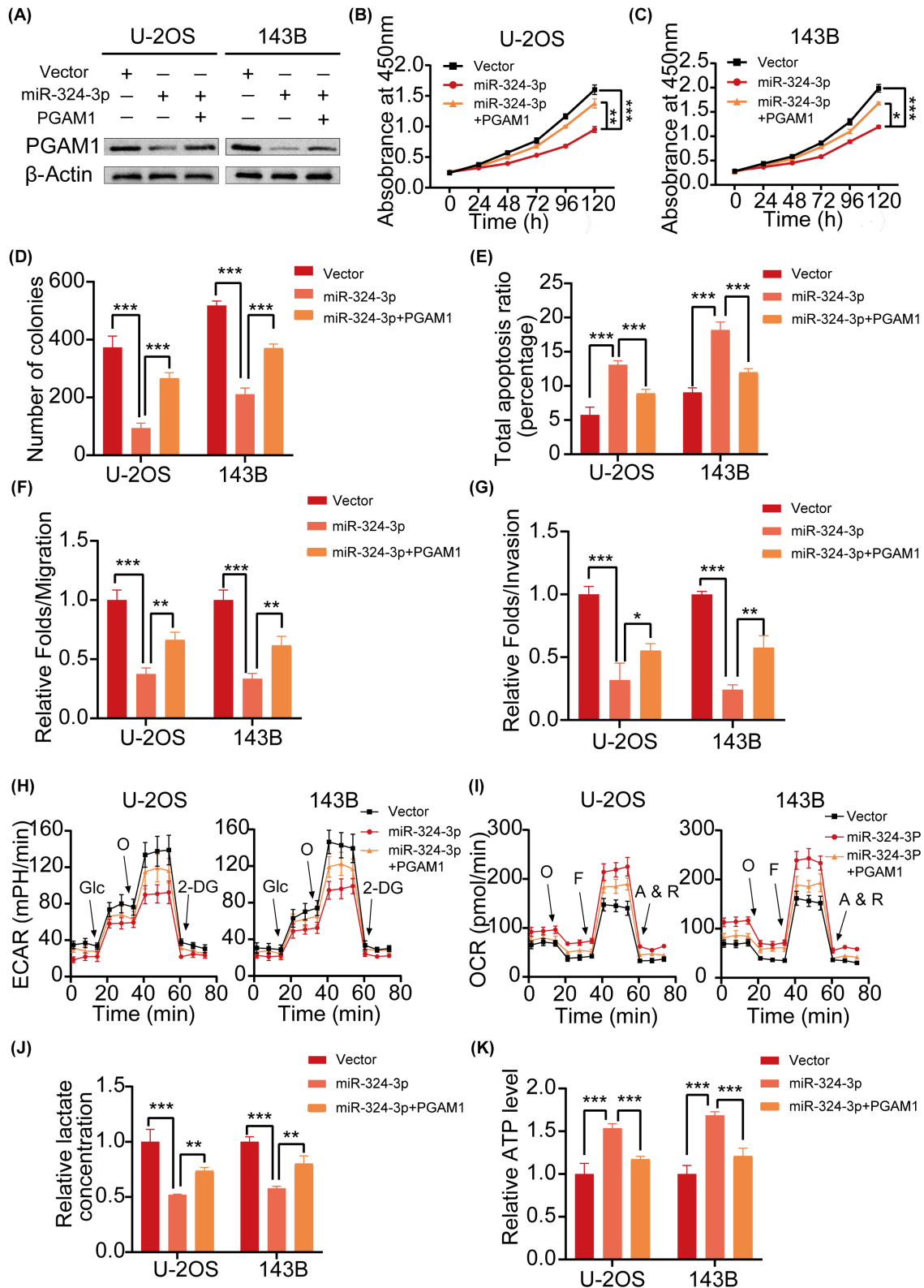


FIGURE 6 Overexpression of phosphoglycerate mutase 1 (PGAM1) partly recovers the oncogenic function of microRNA (miR)-324-3p overexpression in osteosarcoma (OS). (A) Western blot results show PGAM1 expression in OS cells from different groups (negative control, miR-324-3p overexpression, both miR-324-3p and PGAM1 overexpression). (B, C) CCK-8 and (D) colony formation confirmed that the inhibitory effects of miR-324-3p overexpression in OS cells were substantially reduced after enhanced PGAM1 expression. (E) Flow cytometry assays revealed that PGAM1 overexpression partly reversed miR-324-3p-induced apoptosis. (F, G) Migration and invasion ability were measured in different groups. (H, I) Extracellular acidification rates (ECAR) and O_2 consumption rates (OCR) were measured in different groups. (J, K) Lactate production and ATP levels were analyzed in different groups. Results are presented as mean \pm SD. * $p < 0.05$, ** $p < 0.01$, *** $p < 0.001$. 2-DG, 2-deoxy-d-glucose; A&R, antimycin A/rotenone; FCCP, Carbonyl cyanide-p-trifluoromethoxyphenylhydrazone; Glc, glucose; O, oligomycin.

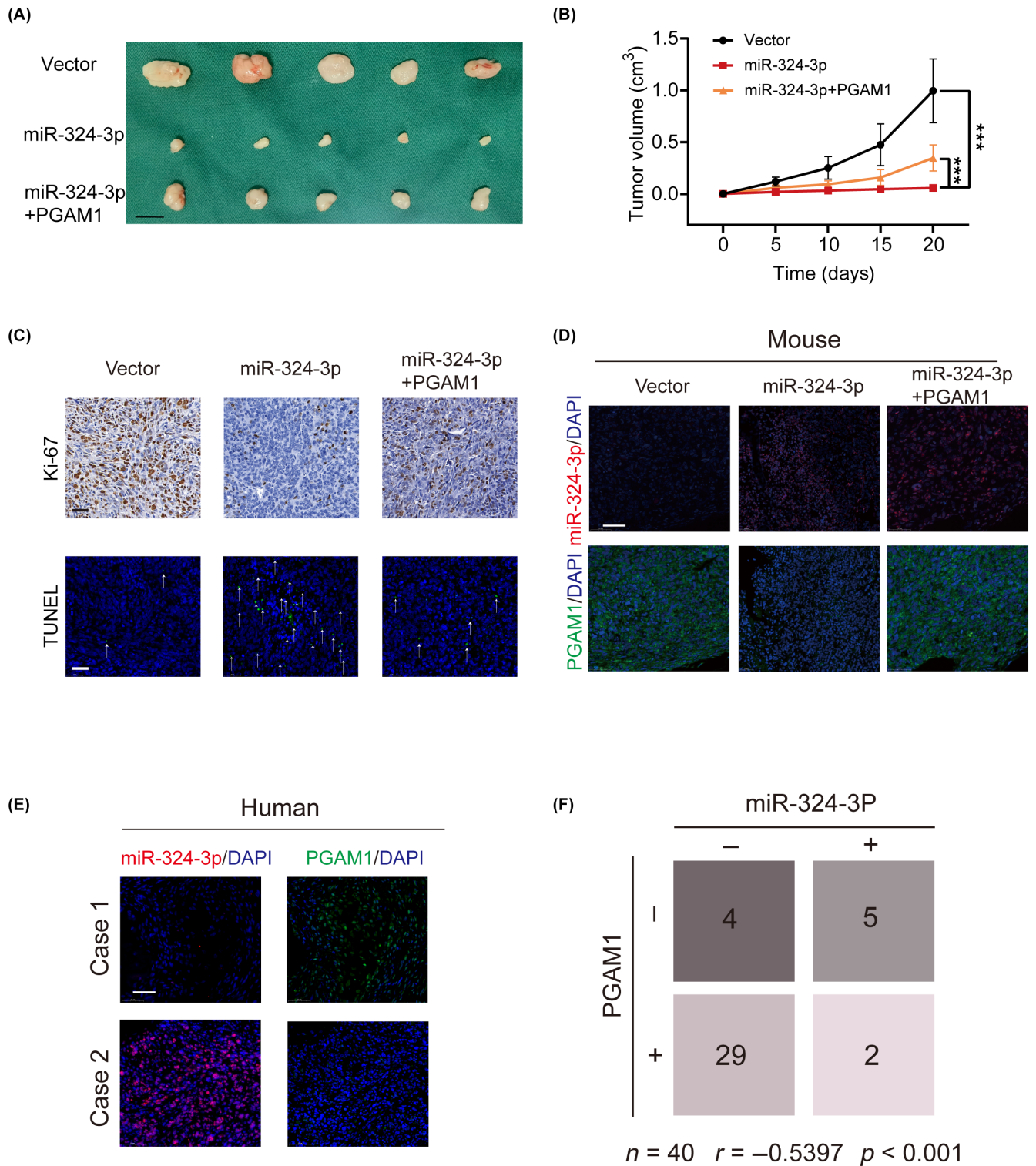


FIGURE 7 MicroRNA (miR)-324-3p/phosphoglycerate mutase 1 (PGAM1) axis is involved in osteosarcoma (OS) growth in vivo. (A) Morphologic characteristics of xenograft tumors from different groups (negative control, miR-324-3p overexpression, both miR-324-3p and PGMA1 overexpression) ($n = 5$). Scale bar, 1 cm. (B) Overexpression of PGAM1 partly reversed the attenuation of tumor induced by miR-324-3p overexpression. Tumors were measured every fifth day. (C) Representative images of Ki-67 and TUNEL staining in xenograft tumor samples from each experimental group of nude mice. Arrows indicate TUNEL-positive cells. (D) Representative photographs of the expression patterns of miR-324-3p and PGAM1 in OS tissues from a subcutaneous xenograft mouse model by immunofluorescence (IF) and FISH. Scale bar, 50 μ m. (E) Representative photographs of the expression patterns of miR-324-3p and PGAM1 in OS tissue microarrays by IF and FISH. Scale bars = 50 μ m. (F) A negative correlation between the expression pattern of miR-324-3p and PGAM1 ($n = 40$, $r = -0.5397$, $p < 0.001$). Results are presented as mean \pm SD. *** $p < 0.001$.

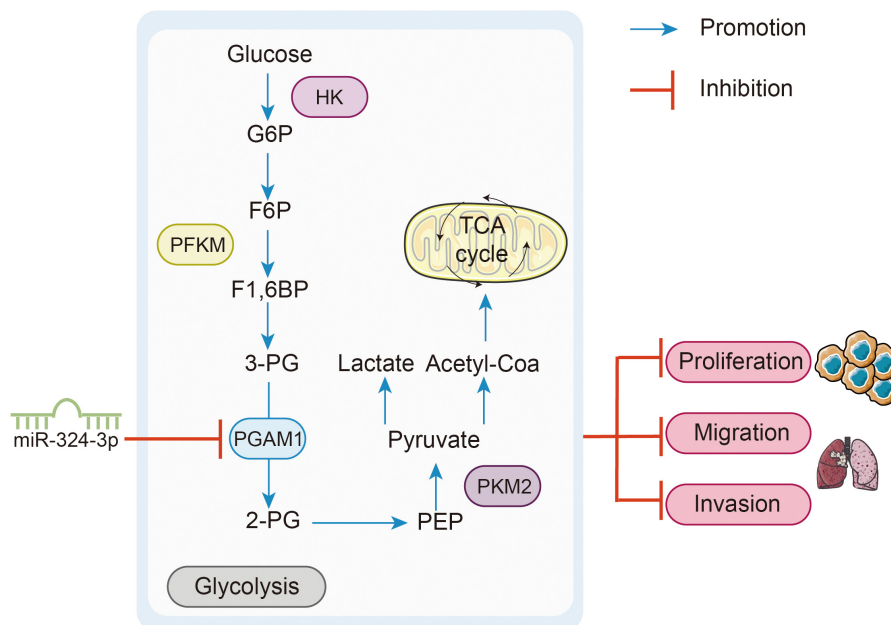


FIGURE 8 Mechanism diagram of the microRNA (miR)-324-3p/phosphoglycerate mutase 1 (PGAM1) axis in osteosarcoma (OS) progression. Ectopic expression of miR-324-3p promoted apoptosis and inhibited OS cell proliferation, migration, and invasion by suppressing PGAM1-mediated glycolysis. 2-PG, 2-phosphoglycerate; 3-PG, 3-phosphoglycerate; F1,6BP, fructose 1,6-bisphosphate; F6P, fructose-6-phosphate; G6P, glucose-6-phosphate; HK, hexokinase; PEP, phosphoenolpyruvate; PFKM, 6-phosphofruktokinase, muscle; PGAM1, phosphoglycerate mutase 1; PKM2, pyruvate kinase M2.

found that the overexpression of miR-324-3p significantly increases mitochondrial respiration and reduces aerobic glycolysis in OS cells.

Notably, the reprogramming of cellular metabolism to maintain deregulated proliferation is a hallmark of cancer cells.³² To sustain rapid growth and proliferation, cancer cells preferentially show much higher glucose uptake and produce a large amount of lactate through enhanced aerobic glycolysis.^{33,34} Hence, targeting aerobic glycolysis has recently been reported to improve tumor growth control and anticancer therapy.³⁵ Previous studies have revealed that the Warburg effect is crucial for OS proliferation, aggressiveness, and drug resistance.^{36,37} Shen et al. reported that CircECE1 regulates the Warburg effect to promote OS growth and metastasis through the c-Myc/TXNIP axis.³⁸ In addition, KCNQ1OT1 promotes OS growth and aerobic glycolysis by functioning as an miR-34c-5p sponge to upregulate aldolase A (ALDOA) expression.³⁹ Moreover, pyruvate kinase M2 (PKM2), a rate-limiting component of the glycolytic pathway, is crucial for OS cell proliferation, invasion, and migration.⁴⁰ In the present study, we identified PGAM1 as a direct and functional target of miR-324-3p, which targets the 3'-UTR of PGAM1.

Phosphoglycerate mutase 1 is a critical enzyme for glycolysis and biosynthesis that converts 3-PG into 2-PG, two key intermediate products in glycolysis.⁴¹ A previous study suggested that PGAM1 plays a vital role in regulating the Warburg effect and anabolic reactions.⁴² Furthermore, PGAM1 inhibition significantly decreases glycolysis in cancer cells and reduces tumor growth.⁴³⁻⁴⁵ Accumulating evidence indicates that PGAM1 is normally upregulated in many types of cancers.⁴⁶⁻⁵⁰ In addition, PGAM1 has been reported to be involved in the Warburg effect in non-small-cell

lung cancers.⁵¹ Moreover, Song et al. revealed that NUDT7 KO affects the glycolytic pathway through the upregulation of PGAM1 expression in articular chondrocytes.⁵² Shen et al. reported that S1P/S1PR3 signaling activated aerobic glycolysis in OS cells by targeting PGAM1.²² The present study provided compelling evidence regarding the possibility that PGAM1 contributes directly to OS tumorigenesis and progression. Furthermore, silencing of PGAM1 potentially inhibited glucose metabolism in OS cells. In addition, PGAM1 overexpression restored the tumor-suppressor effect of miR-324-3p. This finding was further validated in a xenograft model of OS. Accordingly, the findings of the present study led to the speculation that miR-324-3p modulates OS progression and aerobic glycolysis through its inhibitory effects on PGAM1 in vitro and in vivo (Figure 8).

In conclusion, the findings of our study confirm that miR-324-3p is poorly expressed in OS cells and tissues and that miR-324-3p overexpression suppresses OS progression both in vitro and in vivo. Mechanistic studies have revealed that miR-324-3p acts by downregulating PGAM1 and that miR-324-3p inhibits OS progression through PGAM1-mediated aerobic glycolysis. These results offer new insight into the underlying molecular mechanisms of OS and highlight the therapeutic potential of targeting miR-324-3p and PGAM1.

ACKNOWLEDGMENTS

We thank Ruikai Zhou, Shijie Fan, Yadong Tan and Dr. Dong Zhou (Department of Orthopedics, The Affiliated Changzhou Second People's Hospital of Nanjing Medical University, Changzhou Medical Center, Nanjing Medical University, Changzhou, China.) for technical assistance.

FUNDING INFORMATION

This study was supported by Changzhou Sci&Tech Program (CE20215020), the Natural Science Foundation of Xinjiang Uygur Autonomous Region (Grant No. 2022D01F95), and Subject of Changzhou Medical Center of Nanjing Medical University (CMCB202208 and CMCC202217).

CONFLICT OF INTEREST STATEMENT

The authors declare no conflict of interest.

ETHICS STATEMENT

Approval of the research protocol by an Institutional Review Board: The study was approved by the research medical ethics committee of The Affiliated Changzhou Second People's Hospital of Nanjing Medical University.

Informed Consent: N/A.

Registry and the Registration No. of the study/trial: N/A.

Animal Studies: All animal experiments were approved by the Institutional Animal Care and Use Committee of Jiangsu Science Standard Medical Testing Co., Ltd. The ethical approval number is IACUC22-0098.

ORCID

Yifei Shen  <https://orcid.org/0000-0002-1401-7183>

REFERENCES

- Isakoff MS, Bielack SS, Meltzer P, Gorlick R. Osteosarcoma: current treatment and a collaborative pathway to success. *J Clin Oncol*. 2015;33:3029-3035.
- Whelan J, McTiernan A, Cooper N, et al. Incidence and survival of malignant bone sarcomas in England 1979–2007. *Int J Cancer*. 2012;131:E508-E517.
- Gill J, Gorlick R. Advancing therapy for osteosarcoma. *Nat Rev Clin Oncol*. 2021;18:609-624.
- Harrison DJ, Geller DS, Gill JD, Lewis VO, Gorlick R. Current and future therapeutic approaches for osteosarcoma. *Expert Rev Anticancer Ther*. 2018;18:39-50.
- Meltzer PS, Helman LJ. New horizons in the treatment of osteosarcoma. *N Engl J Med*. 2021;385:2066-2076.
- Bartel DP. MicroRNAs: genomics, biogenesis, mechanism, and function. *Cell*. 2004;116:281-297.
- He L, Hannon GJ. MicroRNAs: small RNAs with a big role in gene regulation. *Nat Rev Genet*. 2004;5:522-531.
- Rupaimoole R, Slack FJ. MicroRNA therapeutics: towards a new era for the management of cancer and other diseases. *Nat Rev Drug Discov*. 2017;16:203-222.
- Lee YS, Dutta A. MicroRNAs in cancer. *Annu Rev Pathol*. 2009;4:199-227.
- Hayes J, Peruzzi PP, Lawler S. MicroRNAs in cancer: biomarkers, functions and therapy. *Trends Mol Med*. 2014;20:460-469.
- Ram Kumar RM, Boro A, Fuchs B. Involvement and clinical aspects of MicroRNA in osteosarcoma. *Int J Mol Sci*. 2016;17:877.
- Weng Y, Shen Y, He Y, et al. The miR-15b-5p/PDK4 axis regulates osteosarcoma proliferation through modulation of the Warburg effect. *Biochem Biophys Res Commun*. 2018;503:2749-2757.
- Deng SH, Wu DM, Li L, et al. miR-324-3p reverses cisplatin resistance by inducing GPX4-mediated ferroptosis in lung adenocarcinoma cell line A549. *Biochem Biophys Res Commun*. 2021;549:54-60.
- Liu C, Li G, Yang N, et al. miR-324-3p suppresses migration and invasion by targeting WNT2B in nasopharyngeal carcinoma. *Cancer Cell Int*. 2017;17:2.
- Hsu PP, Sabatini DM. Cancer cell metabolism: Warburg and beyond. *Cell*. 2008;134:703-707.
- Koppenol WH, Bounds PL, Dang CV. Otto Warburg's contributions to current concepts of cancer metabolism. *Nat Rev Cancer*. 2011;11:325-337.
- Vander Heiden MG, Cantley LC, Thompson CB. Understanding the Warburg effect: the metabolic requirements of cell proliferation. *Science*. 2009;324:1029-1033.
- Icard P, Shulman S, Farhat D, Steyaert JM, Alifano M, Lincet H. How the Warburg effect supports aggressiveness and drug resistance of cancer cells? *Drug Resist Updat*. 2018;38:1-11.
- Zhao SJ, Shen YF, Li Q, et al. SLIT2/ROBO1 axis contributes to the Warburg effect in osteosarcoma through activation of SRC/ERK/c-MYC/PFKFB2 pathway. *Cell Death Dis*. 2018;9:390.
- Fong MY, Zhou W, Liu L, et al. Breast-cancer-secreted miR-122 reprograms glucose metabolism in premetastatic niche to promote metastasis. *Nat Cell Biol*. 2015;17:183-194.
- Guo W, Qiu Z, Wang Z, et al. MiR-199a-5p is negatively associated with malignancies and regulates glycolysis and lactate production by targeting hexokinase 2 in liver cancer. *Hepatology*. 2015;62:1132-1144.
- Shen Y, Zhao S, Wang S, et al. S1P/S1PR3 axis promotes aerobic glycolysis by YAP/c-MYC/PGAM1 axis in osteosarcoma. *EBioMedicine*. 2019;40:210-223.
- Bartrons R, Caro J. Hypoxia, glucose metabolism and the Warburg's effect. *J Bioenerg Biomembr*. 2007;39:223-229.
- Kuo WT, Yu SY, Li SC, et al. MicroRNA-324 in human cancer: miR-324-5p and miR-324-3p have distinct biological functions in human cancer. *Anticancer Res*. 2016;36:5189-5196.
- Zhang N, Zeng X, Sun C, et al. LncRNA LINC00963 promotes tumorigenesis and Radioresistance in breast cancer by sponging miR-324-3p and inducing ACK1 expression. *Mol Ther Nucleic Acids*. 2019;18:871-881.
- Shi X, Huo J, Gao X, Cai H, Zhu W. A newly identified lncRNA H1FX-AS1 targets DACT1 to inhibit cervical cancer via sponging miR-324-3p. *Cancer Cell Int*. 2020;20:358.
- Fan C, Yuan Q, Liu G, et al. Long non-coding RNA MALAT1 regulates oxaliplatin-resistance via miR-324-3p/ADAM17 axis in colorectal cancer cells. *Cancer Cell Int*. 2020;20:473.
- Sun GL, Li Z, Wang WZ, et al. miR-324-3p promotes gastric cancer development by activating Smad4-mediated Wnt/beta-catenin signaling pathway. *J Gastroenterol*. 2018;53:725-739.
- Meng H, Guo K, Zhang Y. Effects of lncRNA LINC01320 on proliferation and migration of pancreatic cancer cells through targeted regulation of miR-324-3p. *J Healthc Eng*. 2021;2021:4125432-4125412.
- Geng L, Wang Z, Tian Y. Down-regulation of ZNF252P-AS1 alleviates ovarian cancer progression by binding miR-324-3p to down-regulate LY6K. *J Ovarian Res*. 2022;15:1.
- Xu J, Ai Q, Cao H, Liu Q. MiR-185-3p and miR-324-3p predict Radiosensitivity of nasopharyngeal carcinoma and modulate cancer cell growth and apoptosis by targeting SMAD7. *Med Sci Monit*. 2015;21:2828-2836.
- Pavlova NN, Thompson CB. The emerging hallmarks of cancer metabolism. *Cell Metab*. 2016;23:27-47.
- Lunt SY, Vander Heiden MG. Aerobic glycolysis: meeting the metabolic requirements of cell proliferation. *Annu Rev Cell Dev Biol*. 2011;27:441-464.
- Liberti MV, Locasale JW. The Warburg effect: how does it benefit cancer cells? *Trends Biochem Sci*. 2016;41:211-218.
- Stine ZE, Schug ZT, Salvino JM, Dang CV. Targeting cancer metabolism in the era of precision oncology. *Nat Rev Drug Discov*. 2022;21:141-162.
- Hu XK, Rao SS, Tan YJ, et al. Fructose-coated angstrom silver inhibits osteosarcoma growth and metastasis via promoting

- ROS-dependent apoptosis through the alteration of glucose metabolism by inhibiting PDK. *Theranostics*. 2020;10:7710-7729.
37. Zhang Q, Wu J, Zhang X, Cao L, Wu Y, Miao X. Transcription factor ELK1 accelerates aerobic glycolysis to enhance osteosarcoma chemoresistance through miR-134/PTBP1 signaling cascade. *Aging*. 2021;13:6804-6819.
 38. Shen S, Yao T, Xu Y, Zhang D, Fan S, Ma J. CircECC1 activates energy metabolism in osteosarcoma by stabilizing c-Myc. *Mol Cancer*. 2020;19:151.
 39. Shen Y, Xu J, Pan X, et al. LncRNA KCNQ1OT1 sponges miR-34c-5p to promote osteosarcoma growth via ALDOA enhanced aerobic glycolysis. *Cell Death Dis*. 2020;11:278.
 40. Yuan Q, Yu H, Chen J, Song X, Sun L. Knockdown of pyruvate kinase type M2 suppresses tumor survival and invasion in osteosarcoma cells both in vitro and in vivo. *Exp Cell Res*. 2018;362:209-216.
 41. Vander Heiden MG, Locasale JW, Swanson KD, et al. Evidence for an alternative glycolytic pathway in rapidly proliferating cells. *Science*. 2010;329:1492-1499.
 42. Jiang X, Sun Q, Li H, Li K, Ren X. The role of phosphoglycerate mutase 1 in tumor aerobic glycolysis and its potential therapeutic implications. *Int J Cancer*. 2014;135:1991-1996.
 43. Engel M, Mazurek S, Eigenbrodt E, Welter C. Phosphoglycerate mutase-derived polypeptide inhibits glycolytic flux and induces cell growth arrest in tumor cell lines. *J Biol Chem*. 2004;279:35803-35812.
 44. Evans MJ, Saghatelian A, Sorensen EJ, Cravatt BF. Target discovery in small-molecule cell-based screens by in situ proteome reactivity profiling. *Nat Biotechnol*. 2005;23:1303-1307.
 45. Usuba T, Ishibashi Y, Okawa Y, Hirakawa T, Takada K, Ohkawa K. Purification and identification of monoubiquitin-phosphoglycerate mutase B complex from human colorectal cancer tissues. *Int J Cancer*. 2001;94:662-668.
 46. Ren F, Wu H, Lei Y, et al. Quantitative proteomics identification of phosphoglycerate mutase 1 as a novel therapeutic target in hepatocellular carcinoma. *Mol Cancer*. 2010;9:81.
 47. Peng XC, Gong FM, Chen Y, et al. Proteomics identification of PGAM1 as a potential therapeutic target for urothelial bladder cancer. *J Proteomics*. 2016;132:85-92.
 48. Huang K, Liang Q, Zhou Y, et al. A novel allosteric inhibitor of phosphoglycerate mutase 1 suppresses growth and metastasis of non-small-cell lung cancer. *Cell Metab*. 2019;30(1107-19):1107-1119.
 49. Wen CL, Huang K, Jiang LL, et al. An allosteric PGAM1 inhibitor effectively suppresses pancreatic ductal adenocarcinoma. *Proc Natl Acad Sci U S A*. 2019;116:23264-23273.
 50. Gao H, Yu B, Yan Y, et al. Correlation of expression levels of ANXA2, PGAM1, and CALR with glioma grade and prognosis. *J Neurosurg*. 2013;118:846-853.
 51. Sun Q, Li S, Wang Y, et al. Phosphoglyceric acid mutase-1 contributes to oncogenic mTOR-mediated tumor growth and confers non-small cell lung cancer patients with poor prognosis. *Cell Death Differ*. 2018;25:1160-1173.
 52. Song J, Baek JJ, Chun CH, Jin EJ. Dysregulation of the NUDT7-PGAM1 axis is responsible for chondrocyte death during osteoarthritis pathogenesis. *Nat Commun*. 2018;9:3427.

SUPPORTING INFORMATION

Additional supporting information can be found online in the Supporting Information section at the end of this article.

How to cite this article: Weng Y, Duan W, Yu X, et al. MicroRNA-324-3p inhibits osteosarcoma progression by suppressing PGAM1-mediated aerobic glycolysis. *Cancer Sci*. 2023;114:2345-2359. doi:[10.1111/cas.15779](https://doi.org/10.1111/cas.15779)